II

Electron and band structure in regular or disordered 3-dimensional environments: localised and delocalised states

I Introduction

Calculations based on 3-D environments, using weak bonding approximations, follow much the same line as the studies made in 1-D. The dispersion curve $E = f(k)$ can be traced depending on the different directions under consideration (k_x, k_y and k_z for a cubic crystal). If these directions are not equivalent, and have a forbidden energy for which the value is direction dependent, then the resulting energy gap in the material is of the form.

$E_G = (E_C)_{min} - (E_v)_{max}$ in which $(E_C)_{min}$ corresponds to the minimum conduction band (CB) for all directions $\vec{k}$ considered, and $(E_v)_{max}$ corresponds to the maximum valence band (VB) over all directions.

This approximation for the weak bond is, in fact, only applicable to metals. In this Chapter, we shall look at the electronic bands found within 3-D organic solids and see that their intrinsic semiconducting or insulating character can only be realised by considering strong bonding. We shall also consider 3-D regularly networked solids, considering each node an atom which contributes to the electronic properties of the material, *via*:

(i) a single, s-state electron, and using as example the cubic network to determine the height of the permitted band, otherwise known as the VB.
(ii) hybridised electrons using the specific example of diamond, in which each carbon atom is at the centre of a tetrahedron and has sp^3 hybridised bonding states (as detailed in Appendix A-1, Section II-2); the generation of the band structure and the forbidden band, which separates bands corresponding to bonding and anti-bonding states, will be described.

Finally, we will look at amorphous materials.

II Going from 1-D to 3-D: band structure of networked atoms with single, participating s-orbitals (including simple cubic and face centred systems)

1 3-D General expression of permitted energy

To simplify eqn (22) in Chapter I, which relates the energy of a strongly bonded electron in 1-D, we can rewrite it as

$$E = E_0 - \alpha - \beta \sum_{t=-1,+1} e^{-ikta} \tag{1}$$

The sum is for one atom and its two closest neighbours. On considering more than one dimension though, a simple way of writing eqn (1) is

$$E = E_0 - \alpha - \beta \sum_{m} e^{-i\vec{k}\vec{a_m}}, \tag{2}$$

in which $\vec{a_m}$ represents the vectors joining the reference atom with its m closest neighbours. In the case of a cubic lattice, as shown in Figure II-1, the closest neighbouring atoms have vector $\vec{a_m}$ components:

$$\begin{cases} (\pm a, 0, 0) & \text{in the x axis} \\ (0, \pm a, 0) & \text{in the y axis} \\ (0, 0, \pm a) & \text{in the z axis} \end{cases}$$

The energy thus takes the form $E = E_0 - \alpha - 2\beta[\cos k_x a + \cos k_y a + \cos k_z a]$, in which k_x, k_y, k_z are the components of $\vec{k}$ in the 3 directions Ox, Oy, Oz.

In the centre of the zone, $k = k_0 = 0$ (or $k_x = k_y = k_z = 0$); the energy is minimal and equal to:

$$E = E_0 - \alpha - 6\beta = E(k_0) \tag{3}$$

In the neighbourhood of the central zone, $k \approx k_0 \approx 0$, or $k_x \approx k_y \approx k_z \approx 0$, $\cos k_x a \approx 1 - \frac{(k_x a)^2}{2}$ (ditto for k_y and k_z), and the energy can thus be written as

$$\begin{aligned} E &= E_0 - \alpha - 6\beta + \beta a^2 (k_x^2 + k_y^2 + k_z^2) \\ &= E(k_0) + \beta k^2 a^2. \end{aligned} \tag{4}$$

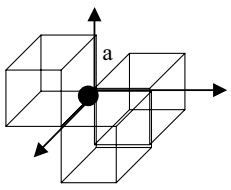

Figure II-1. Geometry of cubic lattice structure.

We can now compare eqn (4) with that obtained by a Mac Laurin development of E using k_0:

$$E_{(k)} = E_{(k_0)} + (k - k_0)\left(\frac{\partial E}{\partial k}\right)_{k_0} + \frac{(k - k_0)^2}{2}\left(\frac{\partial^2 E}{\partial k^2}\right)_{k_0}. \tag{5}$$

As in the centre of the zone, we now have a tangential horizontal (to be compared with Figure I-10), $\left(\frac{\partial E}{\partial k}\right)_{k_0} = 0$ and the mass can be effectively defined by

$$m^* = \frac{\hbar^2}{\left(\frac{\partial^2 E}{\partial k^2}\right)}, \tag{6}$$

so that we can obtain from eqn (5), when $k \approx k_0 = 0$:

$$E_{(k)} = E_{(k_0)} + \frac{\hbar^2}{2m^*}(k - k_0)^2. \tag{7}$$

Again, in the neighbourhood of the central zone, where $k_0 \approx 0$, we now have

$$E_{(k)} = E_{(k_0)} + \frac{\hbar^2}{2m^*}k^2. \tag{7'}$$

Comment: The mass m of an electron can be related in the fundamental dynamic equation $F_T = q(E_{appl} + E_{int}) = m\gamma$ with E_{appl} which is the empirically applied field and γ is the acceleration undertaken by the electron. The internal field (E_{int}) which is derived from the internal potential generated by the nucleus is not well known and the effective mass m^* is defined by the relationship $F_{ext} = qE_{appl} = m^*\gamma$. Eqn (6) is obtained by calculating the work of the external force (see Appendix A-2, Section IV-2).

2 Expressions for effective mass, band size and mobility

The identification of coefficients k^n ($n = 0$ and $n = 2$) of eqns (4) and (7) yields:

$$\begin{cases} E_{(k_0)} = E_0 - \alpha - 6\beta \\ \beta a^2 = \dfrac{\hbar^2}{2m^*}, \quad \text{or} \quad m^* = \dfrac{\hbar}{2\beta a^2}. \end{cases} \tag{8}$$

The size of the band can be deduced from the amplitude of the variation in energy in the first Brillouin zone (described, for 1-D, as the variation in k zone in Figure I-10):

— when $k_x = k_y = k_z = 0$: $E = E(k_0) = E_0 - \alpha - 6\beta$; and
— when $k_x = k_y = k_z = \frac{\pi}{a}$: $E = E(\frac{\pi}{a}) = E_0 - \alpha + 6\beta$.

The amplitude in the variation (4β in 1-D) of E, which is the depth of the permitted band, changes in 3-D to

$$\Delta E = E\left(\frac{\pi}{a}\right) - E(k_0) = B = 12\beta \tag{9}$$

The result given for a simple cubic network can be generalised by introducing a co-ordination number Z, which denotes the number of closest neighbours, and in

our example it is equal to 6 as made evident in Figure II-1. Eqn (9) can thus be rewritten as

$$B = 2Z\beta. \tag{10}$$

Interestingly enough, when mobility is expressed in the form $\mu = \frac{q\tau}{m^*}$, the introduction of β derived from eqn (10) ($\beta = B/2Z$) in eqn (8) gives: $m^* = \frac{\hbar^2}{Ba^2}Z$. In terms of μ, we have

$$\mu = \frac{q\tau a^2}{\hbar^2}\frac{B}{Z}. \tag{11}$$

We can thus conclude that semiconductors have narrow permitted bands as $\Delta E = B$ is small. There is weak coupling between atoms as, following eqn (10), β is also small; in other words, semiconductors display low mobilities.

III 3-D covalent crystal from a molecular model: sp^3 hybrid states at nodal atoms

1 General notes

We will now look at the case of diamond, a material made up of a regular network of sp^3 hybridised carbon atoms. In Appendix A-1, the spatial geometry of bonded carbon is detailed. The bonds are equally spaced when sp^3 hybridisation occurs and the orbitals can be expressed using 4 functions $|\Psi_1>, |\Psi_2>, |\Psi_3>, |\Psi_4>$ as calculated in Appendix A-1, Section III. To follow the formation of the different electronic states and energy levels in diamond, we will sequentially study each step as shown in Figure II-2, by:

a Isolating carbon atoms

Looking at Figure II-2-a and Figure II-2-b, zone (1), we see that the orbitals of isolated carbon atoms, with electronic configuration $1s^2\ 2s^2\ 2p^2$, are characterised by having two levels, E_s and E_p. Note that in Figure II-3, the atoms C, C′, C″ and so on, are assumed to be well separated.

As we bring the C′, C″, C‴, C⁗ closer to the reference atom C, s and p bands form following the superposition of wavefunctions. For example, s-orbitals give rise to bonding and antibonding combinations which tend downwards and upwards, respectively. This is detailed further in Appendix A-2, Section I-2.

b s And p band hybridisation at the critical point M of Figure II-2(a)

When hybridisation of s and p states is energetically favoured, sp^3 states on atom C, described by functions Ψ_1, Ψ_2, Ψ_3 and Ψ_4, are obtained (see Appendix A-1, Section II-2). In the same way, hybrid states of the atom C′ are represented by the functions Ψ'_1, Ψ'_2, Ψ'_3 and Ψ'_4, and so on, for the other C atoms.

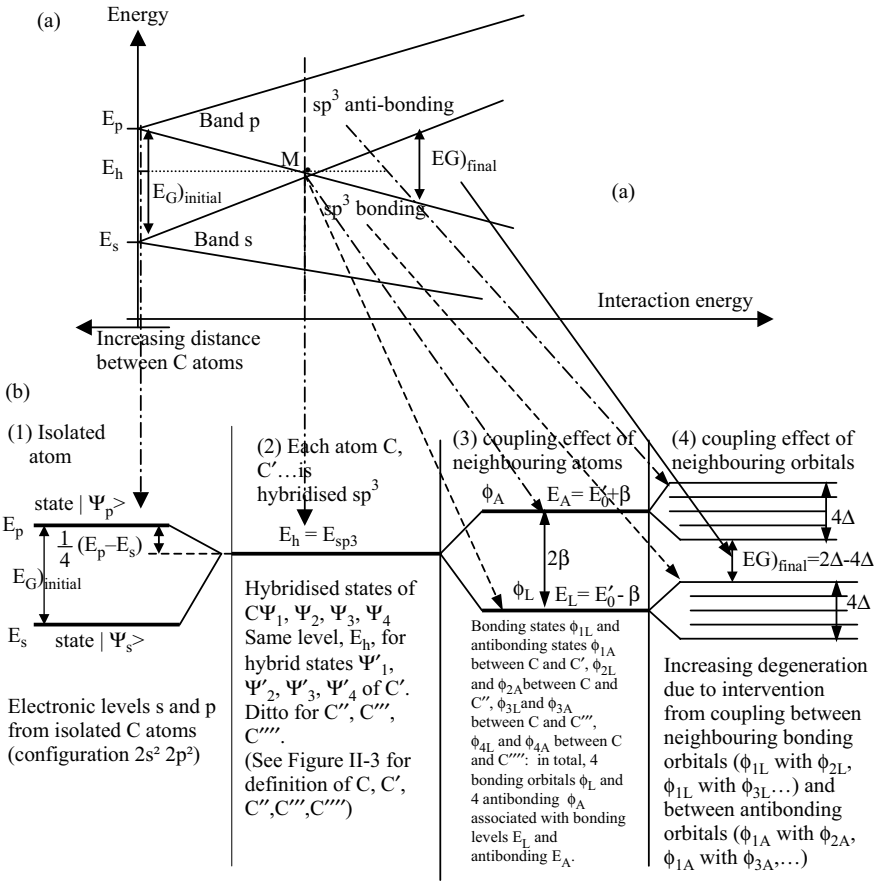

Figure II-2. (a) Band formation due to closing C atoms; (b) evolution in electronic energy levels through successive couplings.

Taking all states together, as shown in zone 2 of Figure II-2(b), and represented by the functions $\Psi_i)_{i=1,2,3,4}$, $\Psi'_i)_{i=1,2,3,4}$ and so on, equivalent to 4N states for a system containing N atoms, we have energy $E_{sp3} = E_{h.}$. E_h can be calculated relatively simply using, for example

$$
\begin{aligned}
E_h &= \langle\Psi_1|H|\Psi_1\rangle \\
&= \left\langle \frac{1}{2}(S + \varphi_{2p_x} + \varphi_{2p_y} + \varphi_{2p_z})|H|\frac{1}{2}(S + \varphi_{2p_x} + \varphi_{2p_y} + \varphi_{2p_z})\right\rangle \\
&= \frac{1}{4}\{\langle S|H|S\rangle + \langle\varphi_x|H|\varphi_x\rangle + \langle\varphi_y|H|\varphi_y\rangle + \langle\varphi_z|H|\varphi_z\rangle\} \\
&= \frac{1}{4}\{E_s + 3E_p\},
\end{aligned}
$$

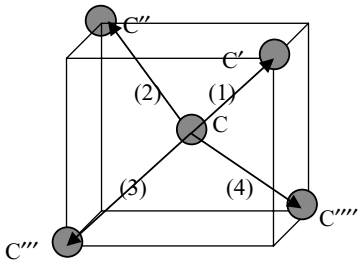

Figure II-3. Relative locations of atoms and available sp^3 couplings.

with

$$E_h = \langle\Psi_2|H|\Psi_2\rangle = \langle\Psi_3|H|\Psi_3\rangle = \langle\Psi_4|H|\Psi_4\rangle = \langle\Psi'_1|H|\Psi'_1\rangle = \cdots = E'_0.$$

E_p and E_s, respectively, represent the energy levels of 2p and 2s states shown in Figure II-2-b. Thus

$$E_p - E_h = E_p - \frac{1}{4}\{E_s + 3E_p\} = \frac{1}{4}(E_p - E_s). \tag{12}$$

c Type A couplings between neighbouring C atoms, as detailed in Figure II-4

Here we consider only couplings (1), (2), (3) and (4), otherwise noted as $C - C'$, $C - C''$, $C - C'''$, $C - C''''$, assuming that interactions that could result from other bonds are negligible. The bonding and anti-bonding states appear as shown in zone 3 in Figure II-2-b. This is detailed, qualitatively, in Section 2 just below.

d Supplementary effects resulting from type B couplings between molecular orbitals, as shown in Figure II-4

Type B couplings are those between (1) and (2), between (2) and (3) and so on, and result in the appearance of energy bands as shown in zone 4 of Figure II-2-b. A quantitative approach is detailed in Section 3 below.

2 Independent bonds: formation of molecular orbitals

Zone (3) in Figure II-2 (b) shows the states which appear following coupling of two sp^3 hybridised orbitals, for example, of C and C′. For this atomic coupling, Φ solutions can be given in the form of a linear combination of each atom's orbitals. As orbital $|\Psi\rangle$ is for atom C, and orbital $|\Psi'\rangle$ is for C′, we now have $\Phi = c|\Psi\rangle + c'|\Psi'\rangle$.

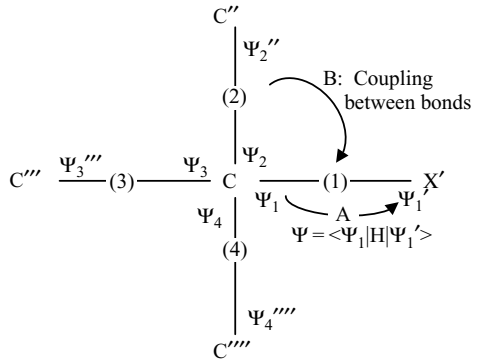

Figure II-4. Representation of successive A and B couplings by projecting plan view of Figure III-3.

On using line (1) in Figure II-4 to indicate the bonding between 2 C atoms, the resulting molecular orbital (Φ_1) can be bonding or anti-bonding (see Appendix A-1);

$$\begin{aligned}\Phi_{1L} &= \frac{1}{\sqrt{2}}(|\Psi_1\rangle + |\Psi_1'\rangle)\\ \Phi_{1A} &= \frac{1}{\sqrt{2}}(|\Psi_1\rangle - |\Psi_1'\rangle)\end{aligned} \tag{13}$$

By taking into account pairs belonging to each carbon atom, and assuming them to be independent, the molecular orbitals which appear about our reference atom C are, in addition to Φ_{1L} and Φ_{1A}:

$$\Phi_{2L} = \frac{1}{\sqrt{2}}(|\Psi_2\rangle + |\Psi_2''\rangle) \quad \text{and} \quad \Phi_{2A} = \frac{1}{\sqrt{2}}(|\Psi_2\rangle - |\Psi_2''\rangle)$$

$$\Phi_{3L} = \frac{1}{\sqrt{2}}(|\Psi_3\rangle + |\Psi_3'''\rangle) \quad \text{and} \quad \Phi_{3A} = \frac{1}{\sqrt{2}}(|\Psi_2\rangle - |\Psi_3'''\rangle)$$

$$\Phi_{4L} = \frac{1}{\sqrt{2}}(|\Psi_2\rangle + |\Psi_4''''\rangle) \quad \text{and} \quad \Phi_{4A} = \frac{1}{\sqrt{2}}(|\Psi_2\rangle - |\Psi_4''''\rangle)$$

The energy levels E_L and E_A are, respectively, associated with bonding and anti-bonding states. They have the same form as that determined in Appendix A-1, that is:

$$\begin{aligned}E_L &= E_0' - \beta \text{ and}\\ E_A &= E_0' + \beta.\end{aligned} \tag{14}$$

Note that $E_0' = H_{ii} = \langle\Psi_i|H|\Psi_i\rangle = E_h = E_{sp3}$ and that the coupling parameter between two atoms under consideration is $-\beta = H_{ii'} = \langle\Psi_i|H|\Psi_i'\rangle$.

Comment For N atoms in a crystal, the number of bonds of type Φ_L is 2N as each carbon atom presents 4 possible bonds each containing 2 electrons, and each shared

between 2 atoms. However, the actual number of valence electrons per atom is 4, resulting from $2s^2 2p^2 \rightarrow 2t^4$, in which t represents hybrid states, and therefore the fundamental state carries 4N electrons, which can also be written as $2 \times 2N$ (the number of electrons per bond multiplied by the number of bonds). All bonding bonds are therefore full when the symmetrically numbered anti-bonding bonds, Φ_A, are empty.

3 Coupling of molecular orbitals and band formation

For a crystal containing N atoms, following the reasoning of Section 2, the energy level E_L (and E_A) is degenerate 2N times, corresponding to 2N bonding orbitals. We will now look at the effect of coupling between different molecular bonds on the degeneration of energy levels.

a Effect of coupling energy between hybrid orbitals on the same carbon atom

The coupling energy between two hybrid atoms is of the form: $\langle \Psi_1 | H | \Psi_2 \rangle = -\Delta$. In terms of either Ψ_1 and Ψ_2 (given in Appendix A-1, Section II-2-c):

$$-\Delta = \left\langle \frac{1}{2}(S + X + Y + Z|H|\frac{1}{2}(S - X - Y + Z) \right\rangle$$
$$= \frac{1}{4}(E_s - E_p - E_p + E_p) = \frac{1}{4}(E_s - E_p).$$

We can see that the effect is not zero and that we should therefore expect, for a covalently bonded 3-D crystal, a non-zero coupling effect between molecular orbitals bonding two adjacent atoms.

b Coupling effects between neighbouring bonding orbitals within a crystal matrix

The coupling within the crystal matrix, shown as B in Figure II-4, corresponds to the form

$$\langle \Phi_{1L} | H | \Phi_{2L} \rangle = \left\langle \frac{1}{\sqrt{2}}(|\Psi_1\rangle + |\Psi_1'\rangle)|H|\frac{1}{\sqrt{2}}(|\Psi_2\rangle + |\Psi_2''\rangle) \right\rangle.$$

Ignoring coupling integrals between non-adjacent electrons, as for example $\langle \Psi_1' | H | \Psi_2 \rangle \approx 0$, results in:

$$\langle \Phi_{1L} | H | \Phi_{2L} \rangle = \frac{1}{2}\langle \Psi_1 | H | \Psi_2 \rangle = \frac{1}{2} \times \frac{1}{4}(E_s - E_p) = -\frac{\Delta}{2}. \quad (15)$$

On modifying energy levels of type E_L, coupling of molecular bonds results in an increased degeneration to the level of $E_L = E_0' - \beta$.

By analogy to the 1-D system looked at in Chapter 1, wavefunctions of the crystal must be written in the form of a linear combination of either bonding orbitals, Φ_L, or

of anti-bonding orbitals, Φ_A. These functions, which are characteristic of a regular network, should also satisfy Bloch's theorem and are thus of the form:

$$\left|\Phi_k^L(\vec{r})\right\rangle = c_0 \sum_s e^{i\vec{k}\cdot\vec{r}_s} \left|\Phi_L(\vec{r}-\vec{r}_s)\right\rangle$$

$$\left|\Phi_k^A(\vec{r})\right\rangle = c'_0 \sum_s e^{i\vec{k}\cdot\vec{r}_s} \left|\Phi_A(\vec{r}-\vec{r}_s)\right\rangle$$

These are the Bloch sums for bonding and anti-bonding orbitals, and are for electrons delocalised throughout a whole crystal network in 3-D. They are similar to the wavefunctions used in 1-D to verify Floquet's theory (eqn (10) of Chapter I).

In the same way as that observed for s-orbitals in a 1-D system (Chapter 1) and in a 3-D system (Section II-1 of this Chapter), the functions result in a fragmentation of E_L and E_A levels, as shown in going from zone 3 to zone 4 in Figure II-2. We thus obtain $2N\left|\Phi_k^L(\vec{r})\right\rangle$ functions. Having taken into account 4N spin functions we now have a full band of bonding states, justifying the term "Highest Occupied Molecular Orbital" (HOMO), otherwise known as the valence band by physicists. The band of anti-bonding states though is empty and is known as the "Lowest Unoccupied Molecular Orbital", or for physicists, the conducting band. The pair of bands are separated by what is known as the "band gap" of height E_G.

Quantitatively, we have seen in Section II of this Chapter that for s-orbitals characterised by a coupling parameter $-\beta = \langle\psi_s|H|\psi_{s\pm1}\rangle$), the size of the formed bands is equal to $2Z\beta$ (eqn (10) of Section II). In the case of Figure II-4 treated here, the co-ordination number (Z) equals 4 and the coupling parameter, $\langle\Phi_{1L}|H|\Phi_{2L}\rangle = -\frac{\Delta}{2}$. The size of the HOMO and LUMO bands is therefore, following eqn (10), $B = 2.4$. $\frac{\Delta}{2} = 4\Delta$ (zone (4) of Figure II-2-b). In addition, the height of the band gap can be calculated directly from Figure II-2-b using $E_G = 2\beta - 4\Delta$. The values of β and Δ depend on the network and size of atoms. With diamond having a band gap of around 5.4 eV, it is more of an insulator than a semiconductor. On descending down through column IV of the periodic table, moving from carbon, through silicon to germanium, the size of the atoms increases and the size of the permitted bands also increases to the order of *ca.* 4Δ. With each successive increase in atom size, the band gap diminishes: C, 5.4 eV; Si, 1.1 eV; and Ge, 0.7 eV.

IV Band theory limits and the origin of levels and bands from localised states

1 Influence of defaults on evolution of band structure and the introduction of 'localised levels'

Figure II-5 continues on from Figure II-2-b by considering the origin of the VB and CB for a perfectly ordered system of tetrahedral carbon atoms. As we have seen, the initial s^2p^2 configuration gives rise to 4 sp^3 type molecular orbitals. And each one of

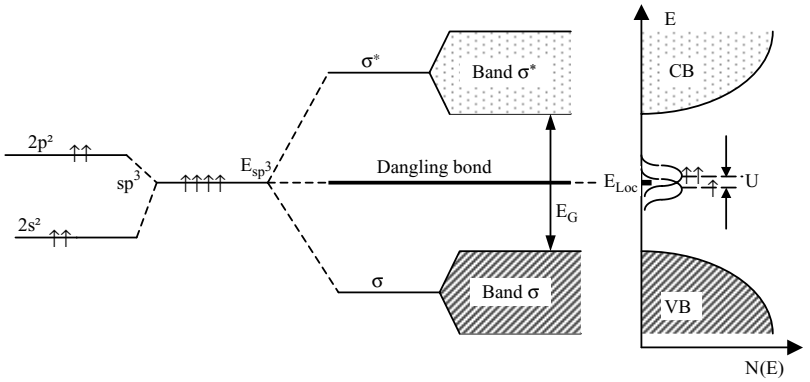

Figure II-5. Origin of localised levels associated with dangling bonds of tetrahedral carbon.

these leads to the formation of a bonding σ-orbital and an anti-bonding σ*-orbital. In going from single molecules to the solid state, the combination of sp^3 orbitals leads to the rupture of σ- and anti-bonding σ*-orbitals into valence and conduction bands, respectively.

Because of the finite size of a real crystal, however, at the surfaces faults occur as each carbon atom is bonded to 3 rather than 4 carbon atoms. This results in one incomplete sp^3 bond, or "dangling" bond, which contains one electron and, intrinsically, is electrically neutral. The single electron is situated at the level E_{sp3}, even if the localised level associated with the electron is E_{Loc}, and is in the middle of the band gap, given the permitted bands allowed (Figure II-5).

Other faults can give rise to similar levels in a real crystal: vacated sites (generated during the preparation of the crystal); and dangling bonds induced by physical treatment, such as irradiation or ion implantation which, breaks bonds as the crystal is traversed.

The presence of structural faults, caused by dangling bonds, can create disorder, for example fluctuations in bonding angles, and result in an opening of levels and the formation of a default band. The exact positioning of the bands relies on relaxation phenomena which occur in the solid following fault formation, and whether they result from valence or conduction bands.

In Figure II-5, the lower band, near the middle of the band gap, corresponds to a dangling bond containing one electron. It is therefore a donor type band which is neutral and in an occupied state. The upper band, near the middle of the band gap, corresponds to the same fault but has a different charge *i.e.* has received an extra electron, and is an acceptor band which would be neutral if it were empty (see page 344 of [Ell 90]). The energy difference between these two types of faults, of which one is neutral when it is full, the other neutral when it is empty, corresponds to the Hubbard correlation energy (U), for which $U = \langle q^2/4\pi\varepsilon_0\varepsilon_r r_{12}\rangle$, in which r_{12} designates the average distance between two electrons on the same site over all possible configurations.We

will now go on to try and detail the effects resulting from these electronic repulsions which up until now have been treated as negligible.

2 The effects of electronic repulsions, Hubbard's bands and the insulator-metal transition

In band theory, until now, we have considered that each electron existed in an average potential resulting from a collection of atoms and other electrons. In the case of alkali metals (Li, Na, K. . .), which have one free electron per atom, the transfer of an electron from one atom to its neighbour through a conduction band occurs *via* electronic levels situated just above the Fermi level (E_F) and the energy utilised is extremely small, of the order of a fraction of a meV.

a The model

In utilising Hubbard's model and theories, we can consider that the only important electronic repulsions are those which occur between two electrons which are on the same site (the same atom in a series of alkali metal atoms). The repulsion energy, or Hubbard energy, can be evaluated to ascertain if it is significant for certain materials and can even help indicate the origin of certain metal-insulator transitions. As before, we will use the same chain of alkali metals as shown in Figure II-6-a to evaluate the problem, although we will assume that overlapping between atoms is poor and the transport of electrons from one atom to the next requires a great deal of energy. Movement of an electron thus generates a supplementary repulsive energy which can be estimated by:

— calculating the ionisation energy required (I_p) to separate an electron from the atom A'_1 to which it is attached which subsequently becomes A_1 (this change is shown in going from Figure II-6-a to Figure II-6-b); and

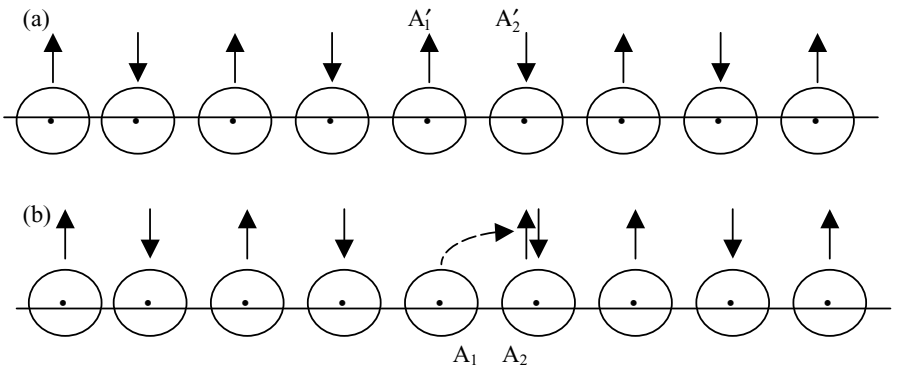

Figure II-6. Highlighting electronic repulsions in a chain of atoms with s-orbitals.

— calculating the energy recovered, or the electron affinity (χ) when the free electron is placed on the independent, adjacent atom A_2', which subsequently becomes A_2.

The total energy thus required, equivalent to the repulsive energy, is $U_H = I_p - \chi$.

For hydrogen $I_p = 13.6\,eV$ and $\chi = 0.8\,eV$, and thus $U_H = 12.8\,eV$, showing how U_H can attain a relatively high value of several eV.

Elsewhere, Mott showed how the repulsive energy can be calculated using r_{12} [Mot 79], which represents the distance between two electrons on the same site or atom, and $\psi(r)$ which is the wavefunction corresponding to the value proposed at the end of the preceding Section 1.

$$U_H = \int\int \frac{e^2}{4\pi\varepsilon_0 r_{12}} |\psi(r_1)|^2 \, |\psi(r_2)|^2 \, dr_1 dr_2.$$

Practically speaking, this energy is particularly important with respect to transition metal oxides, such as NiO, for which electron transport occurs *via* d-orbitals and can be written as:

$$Ni^{2+} + Ni^{2+} \longrightarrow Ni^{3+} + Ni^{+}$$

For a chain of alkali metals, however, the same electron transfer, *via* s-orbitals, is written:

$$Cs + Cs \longrightarrow Cs^{+} + Cs^{-}$$

In Figure II-6, $A_1' \equiv A_2' \equiv Cs$ while $A_1 \equiv Cs^+$ and $A_2 \equiv Cs^-$. On removing the arrows in Figure II-6, which represent the division of electrons throughout a chain of atoms, we can consider that for NiO, $A_1' \equiv A_2' \equiv Ni^{2+}$, $A_1 \equiv Ni^{3+}$ and $A_2 \equiv Ni^{+}$. Placing an electron on a Ni^{2+}, to form a Ni^{+} ion, would require the energy given by $U_H = I - \chi$ if the Ni^{+} and Ni^{3+} ions, at positions A_2 and A_1 in Figure II-6-b, respectively, are sufficiently far apart. The transported electron can be assumed to pass through a free state, that is its energy E_n at the level $n \to \infty$ tends towards 0, as do the successive energies I_p and $-\chi$, as previously described.

Energy levels of isolated ions can be represented in terms of $-I_p$ (the energy of an orbital which looses an electron, *i.e.* Ni^{3+} or A_1) and $-\chi$ (the energy of a supplementary electron situated on Ni^{+} or A_2). When the ions are well separated, as shown in the far left part of Figure II-7, each energy level is separated by $U_H = I_p - \chi$ which appears as a band gap between the upper and lower levels, the former having received an electron, the latter having lost one.

On bringing the ions closer to one another, as described in going from the left to right side of Figure II-7, transport by charge carriers becomes possible *via* the permitted bands which start to form. These newly formed discrete bands give rise to permitted bands (Hubbard's bands), upper level bands of electrons (in which Ni^{+} can be found) and lower level bands containing holes (in which Ni^{3+} resides).

As the size (B) of the bands grows with increasing proximity of atoms, the difference $U_H - B$ decreases and eventually disappears when B reaches U_H. Beyond this value—obtained when the atoms are close enough to each other—the upper and lower Hubbard bands overlap and the band gap is removed; this point is also known as the Mott-Hubbard transition from an insulator to metallic state.

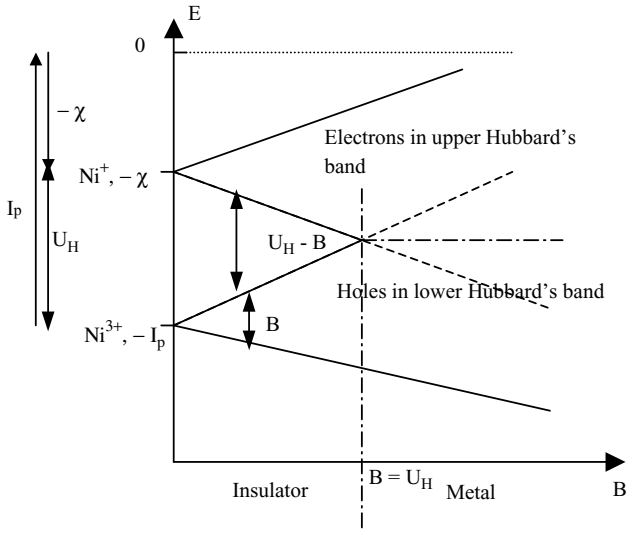

Figure II-7. Evolution of Hubbard bands as a function of band size (B). $B = 0$ for atoms far apart but when $B = U_H$, the band gap $U_H - B$ disappears to give a metal-insulator transition.

b Charge transfer complexes

Charge transfer complexes (CTCs) are materials in which the effective correlation energy is high [And 92]. If the effective energy (U_{eff}) is defined as the difference between the electronic repulsion energy for a site occupied by two electrons (U_o) and the electronic repulsion energy between two electrons on adjacent sites (U_1) *i.e.* $U_{eff} = U_0 - U_1$, then for a CTC the energy U_H corresponds to U_{eff}.

For a system with N sites:

— if we can assume that U_{eff} is negligible, each site can be occupied by two electrons (spin up, ↑, and spin down, ↓). In addition, as in Figure II-8-a, if the system is half filled by N electrons then the material is metallic;

— if the system is one in which U_{eff} is high, we can place only one electron per site. Again, if the system carries N electrons (i.e. $\rho = 1$, in which ρ designates the number of electrons per site) then all energy levels are occupied and the band is full as shown in Figure II-8-b. Only B inter-band transitions are allowed, demanding a high energy of activation (E_a), and the system, in other words, is an insulator (Mott insulator) or semiconductor. For example, the complex HMTTF-$TCNQF_4$, in regular columns, has $\rho = 1$, $E_a = 0.21$ eV with a room temperature conductivity $\sigma_{RT} = 10^{-4}\Omega^{-1}\,cm^{-1}$; and

— once again, if the system is one in which U_{eff} is high and we can only place one electron per site but $\rho < 1$ because bonds at the interior of each column are not fully occupied, both A intra- and B inter-band transitions are possible with the former requiring, respectively, low and high activation energies. This is shown in Figure II-8-c. As an example, $TTF^{+0.59} - TCNQ^{-0.59}$ displays a metallic character with $\rho = 0.59$ and $\sigma_{RT} = 10^{3}\Omega^{-1}\,cm^{-1}$.

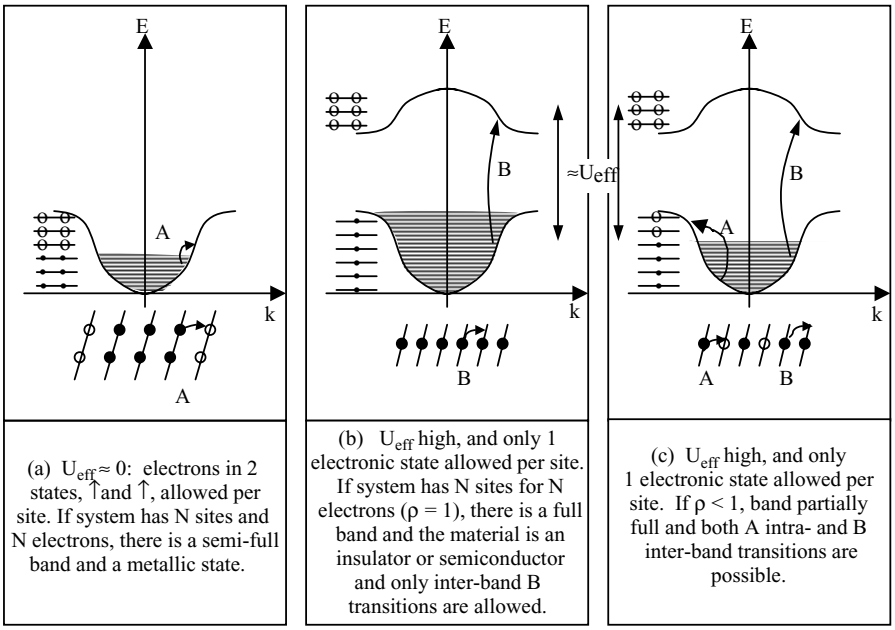

Figure II-8. Electron transport with respect to electronic structure. Upper parts of the Figures represent band schemes and lower parts represent electron positions (• = occupied state, ∘ = empty state).

c The Mott transition from insulator to metal: estimation of critical factors

Different theories have been elaborated to establish, in a quantitative manner, the parameters surrounding transitions from insulator to metallic states. The Thomas-Fermi screened potential can be used [Ell 98], [Sut 93] and the basis of theoretical developments, including the application of magnetism, can be followed up elsewhere [Zup 91]. We will limit ourselves here to saying that this transition can result from competition between localisation effects, themselves resulting from electron Fermi kinetic energies (E_F) and the electrostatic energies to which they are subject.

In order to take into account environmental effects and polarisation, two elements must be considered: the permittivity of the medium under study ($\varepsilon_0\varepsilon_r$)($\varepsilon_r$ being the relative permittivity of the material); and the active length (a^*) of the electrostatic potential, which takes on the form $e^2/4\pi\varepsilon_0\varepsilon_r K_1 a^*$. K_1 is a constant which accounts for the present-day incomplete knowledge of interaction distances, which can be written simply as $K_1 a^*$. It should be noted that a^* must take on the same form as the first Bohr orbit (a_0), that is $a_0 = [\varepsilon_0 h^2]/[\pi m e^2]$. To obtain a^* from a_0, ε_0 needs once again to be replaced by $\varepsilon_0\varepsilon_r$, to take into account the effect of the interaction between network and electron thus changing the latter mass from m to m^* so that $a^* = [\varepsilon_r\varepsilon_0 h^2]/[\pi m^* e^2]$ or $a^* = \varepsilon_r a_0(m/m^*)$.

As $E_F = (\hbar^2/2m^*)(3\pi^2 n)^{2/3} = (K_2 h^2 n^{2/3})/(4\pi^2 m^*)$, in which n is the electron concentration (page 171 of [Mooser 93]) and K_2 a constant, the condition required to reach the metallic state can be written: $(h^2 n^{2/3})_{n=nc}/(4\pi^2 m^*) \geq Ce^2/(4\pi\varepsilon_0\varepsilon_r a^*)$, in which C is, as yet, an unresolved constant resulting from the introduction of the aforementioned constants K_1 and K_2. The relationship is thus based on n_c, at which point the transition occurs. Therefore, we should have $a^* n_c^{2/3} \geq C(e^2 m^* \pi)/(\varepsilon_0\varepsilon_r h^2)$, either in terms of the expressions a^* and a_0, as in $(a^* n_c^{1/3})^2 \geq C$, or expressed as $a^* n_c^{1/3} \geq D$, in which $D = C^{1/2}$. Experimentally, the constant D is normally found to be around 8 times the value of n_c (it has been shown that $D \approx 0.26$) and thus the criteria for the transition is:

$$(a^* n_c^{1/3})^2 \geq 0.26. \tag{16}$$

Physically speaking, this criterion means that all materials can become metallic if they are sufficiently compressed so that the electron density reaches the value n_c. The corresponding metal-insulator transition (M-I transition, which also occurs at $n = n_c$) is called the Mott transition and originates from localisation of electrons through electrostatic interactions, not from any material disorder. We shall see in the following Section 3 how disorder alone can result in the Anderson transition.

d π-Conjugated polymers

Polymers conjugated by π-orbitals are, in principle, not subject to Mott transitions as transfers from one site to another in the same chain have β integral values which are too high (typically of the order of $4\beta \approx 10\,\text{eV}$ for polyacetylene), well above electron-electron interaction energies (U, below 1 eV for polyacetylene). Figure II-8-a therefore sufficiently describes these materials, although they do display insulating characteristics, which in the case of polyacetylene results from a Peierls distortion due to electron-phonon interactions which open the band gap (Figure II-9).

3 Effect of geometrical disorder and Anderson localisation

a Introduction

The effect of geometrical disorder has for the most part been studied within theories on amorphous semiconductors developed by Mott and Davies [Mot 71, Mot 79 and Mot 93], and discussed—in French—by Zuppiroli [Zup 91] and Moliton [Mol 91].

The theory is based on two fundamental ideas:

— the first was taken from the work of Ioffe and Regel [Iof 60] who observed that there was no great discontinuity in the electronic properties of semi-metallic or vitreous materials when going from solid to liquid states. It was concluded that electronic properties of a materials cannot be only due to long range order, as was proposed by Bloch for properties of crystals, but are also determined by atomic and short range properties in which the average free path of an electron is interatomic. It is worth noting also, that even though a material may be amorphous,

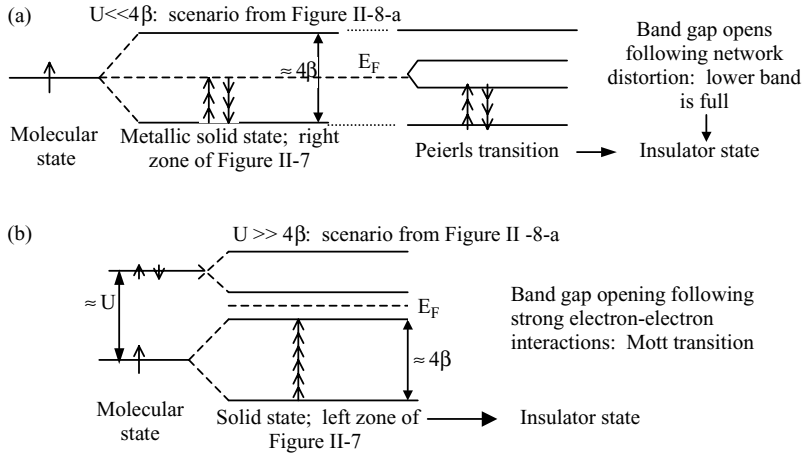

Figure II-9. (a) Characteristics of π-conjugated polymers, with the example of polyacetylene under a Peierls transition, verifying that $U \ll 4\beta$, in contrast with (b) Mott insulators for which $U \gg 4\beta$ (and possible for CTCs).

this does not exclude it from having bands. For example, glass, which is a non-crystalline material, is transparent in the visible region of light ($\approx 1.5 - 3$ eV), that is to say that while absorption of photons with energy below 3 eV does not occur, glass does actually have a band gap of at least greater than 3 eV; and

— the second rests on the evidence given by Anderson [And 58] for a material without long range order that nevertheless have localised states with permitted energy bands for electrons. This theoretical model comes from observations made on certain amorphous semiconductors in which charge carriers cannot move.

b Limits to the applicability of band theory and Ioffe Regel conditions

Bloch functions, *i.e.* $\psi_k(r)$, can be used to describe electron wavefunctions in perfectly crystalline materials. The electronic states are delocalised and spread out over space, as denoted by $|\psi_k(r)|^2$. Because of perfect delocalisation, the average free mean path of an electron can be considered infinite. It is only when studying a real crystal that the average free path of an electron takes on significance because of effects due to quasi-imperfections caused by vibrations, called phonons, and imperfections caused for example by doping agents and impurities which perturb the regularity of potential throughout the network. It is only when these electron scattering effects, which limit the free path of electrons are considered, that the statistical average term $\mathcal{L}$ of the free path length of an electron between two successive collisions can be introduced. In addition, there are two terms to note: "lattice scattering" which indicates collisions due to the material network and for a similar effect caused by ionised impurities, the term "impurity scattering" is used.

On disordering a lattice by introducing vibrations and/or impurities, $\mathcal{L}$ appears and takes on a decreasing value as disorder increases. If there is a low amount of

impurities, then local levels appear, most notably in the forbidden band (FB), but if the number of impurities increases, the localised levels grow to form impurity bands which can reach a size ΔE_e, close to that of the valence band (VB), the conduction band (CB) and the FB introduced in Bloch's theory. Bloch's theory though looses all semblance of reality when values of ΔE_e reach the same values of the bands. Put another way, we can go from the crystalline state to the amorphous state with $\mathcal{L}$ decreasing until Bloch's theory is no longer acceptable. The limit for $\mathcal{L}$ was fixed to $k\mathcal{L} \sim 1$ (for a perfect crystal, $k\mathcal{L} \gg 1$) by Ioffe and Regel by following the reasoning of the uncertainty principle, *i.e.*

$$\Delta E \cdot \Delta t \geq \hbar \quad \text{and} \quad \Delta x \cdot \Delta k \geq 1. \tag{17}$$

To arrive at the result shown above, we can consider that the trajectory of an electron after a collision is random, and at the very best can only be defined between two collisions, *i.e.*:

$$(\Delta t)_{max} = \tau \tag{18}$$

in which τ is the relaxation time—the average time between two collisions; and

$$(\Delta x)_{max} = \mathcal{L} \tag{19}$$

From eqn (17) we can thus directly derive the best precision in ΔE, $(\Delta E)_{min}$, and in Δk, $(\Delta k)_{min}$, when:

1) the equivalence of (17) by ΔE is verified. $\Delta t = \hbar$ and $\Delta x \cdot \Delta k = 1$;
2) when Δt and Δx are at their highest value in the equalities just above and equal to $(\Delta t)_{max} = \tau$ and at $(\Delta x)_{max} = \mathcal{L}$.

We arrive at:

$$(\Delta E)_{min} \cdot \tau \approx \hbar, \tag{20}$$

and

$$(\Delta k)_{min} \cdot \mathcal{L} \approx 1. \tag{21}$$

The question we are therefore brought to ask is with increasing disorder, what are the lowest values that τ (and thus the mobility $\mu = q\tau/m$) and $\mathcal{L}$ can go to while $(\Delta E)_{min}$ and $(\Delta k)_{min}$ retain acceptable values, values which are compatible with classical theory of bands in a real crystal.

The response can be given be using simple calculations which show that when:

- $\mu \to 1\,cm^2\,V^{-1}\,s^{-1}$ (and $\tau \approx 6 \times 10^{-16}$ s), from eqn (20) $(\Delta E)_{min} \approx 1$ eV. Thus, $(\Delta E)_{min} \approx E_G$ (band gap size) or $(\Delta E)_{min}$ is the same order of size as the permitted bands. When $\mu \leq 1\,cm^2\,V^{-1}\,s^{-1}$, incertitude in the energy of the carriers tends to the same order of size as the permitted and forbidden bands, *i.e.* to such an extent such that the band scheme looses its relevance to real systems. It will be shown though that the Anderson model band scheme has to take into account localised bands with a gap which eventually becomes the mobility gap, E_μ.

- $\mathcal{L} \rightarrow$ a few Angstroms, that is to say $\mathcal{L} \approx a$, in which a is the lattice constant and is typically of the order of 3×10^{-8} cm, eqn (21) results in $(\Delta k)_{min} \approx 1/\mathcal{L} \approx 1/a \approx 3 \times 10^{7}\,cm^{-1} \approx k$. In effect, with $\lambda = h/mv$ in which $v = v_{thermal} \approx 100\,km\,s^{-1}$ and $\lambda \approx 7 \times 10^{-7}$ cm, we have $k = 2\pi/\lambda \approx 10^{7}\,cm^{-1}$, and can directly infer that in a band scheme, conduction electrons will be such that $k \approx 1/a$. At these values where $\mathcal{L} \approx a$, we therefore have $(\Delta k)_{min} \approx k$, and k can no longer be considered a good physical parameter to which we can apply quantification. In addition, when $\Delta k \sim k$ Fermi's sphere is so badly defined that it can, at a limit, be totally deformed and the concept of carrier speed looses significance as $\hbar k = m^{*}v$, just as much as the average free path which is expressed as a function of v following $\mathcal{L} = v\tau$.

Finally, as soon as $\mathcal{L} \approx a$, and more strictly speaking as soon as $\mathcal{L} \leq a$ which occurs when the interaction between an electron and the material network becomes increasingly strong, an electron no longer goes any further than the limits of the atom to which is tied. The electronic wavefunction localises over a small region in space and is generally supposed to diminish exponentially with respect to R following $\exp(-\alpha R)$.

Having followed the work of Mott and Anderson, we are brought to a new concept of localised states. The permitted density of states, N(E), always results in an energy band beneath a single E_C for a conduction band and above a single E_V for a valence band, and, in other words, an activation energy is necessary for carriers to pass from one state to another with an emission or absorption of a phonon.

c Anderson localisation

α) *The model* Systems in which disorder is due to a random variation in the energetic depth of regularly spaced sites (with interstitial distances always equal to a) are considered in Anderson's model, and can relate, for example, to a random distribution of impurities. Different authors, including Mott, have tried to take into account lateral, spatial disorder and the results have been close to those of the Anderson model, of which we will limit our discussion to this section.

In Chapter 1, we saw that if we take into account effects resulting from a network of atoms at nodes by constructing a regular distribution of identical potential wells, then a permitted energy band of height B appears, as shown in Figure II-10.

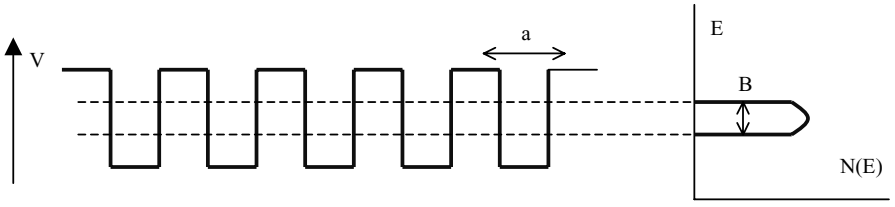

Figure II-10. Regular distribution of identical potential wells and permitted band.

In the approximation of strong bonds, we saw in Section II-1 of this Chapter that:

- $B = 2Z\beta$, with $Z =$ the number of adjacent neighbours and β the resonance integral between two adjacent sites;
- $$m^* = \frac{\hbar^2}{2\beta a^2} = \frac{\hbar^2}{a^2 B} Z \tag{22}$$

  so that $\mu = \frac{q\tau a^2}{\hbar^2}\frac{B}{Z}$, and semiconductors possessing a narrow B band exhibit low mobilities.

For Anderson's model we replace the preceding distribution by one of randomly deep potential wells which represent disorder, as shown in Figure II-11.

β) *Variation in wavefunctions with respect to V_0/B (Anderson) and $\mathcal{L}$ (Ioffe and Regel)*
We will show here how permitted energy bands change into localised states if V_0/B goes beyond its critical value. In order to do this, we need to look at the following, successive scenarios:

— *Real crystal*: V_0/B *is very low and* $\mathcal{L}$ *is high*

Here the wavefunction is given by Floquet's theory (eqn (10) of Chapter 1) which we can write to the order of a normalisation constant:

$$\psi_k(r) = \sum_n e^{ikr_n}\psi_0(r-r_n). \tag{23}$$

The average free path can be estimated from the Born approximation, [page 401 of Smi 61], by realising that the wave vector of an electron (k_n) changes to k_m once the electron has undergone a collision of probability P_{mn} and that $P_{nm} = \frac{1}{\tau} = \frac{V}{\mathcal{L}}$, and in addition [page 16 of Mot 71] P_{nm} is given by Fermi's 'golden rule': $P_{nm} = \frac{1}{4}\frac{2\pi}{\hbar}|\Omega|^2_{moy} N(E_m)$ (eqn (2.20) of [Mol 91] relating to unit volume). For conducting electrons, for which $E_m \approx E_F$, spread throughout a volume $V = a^3$ with a random

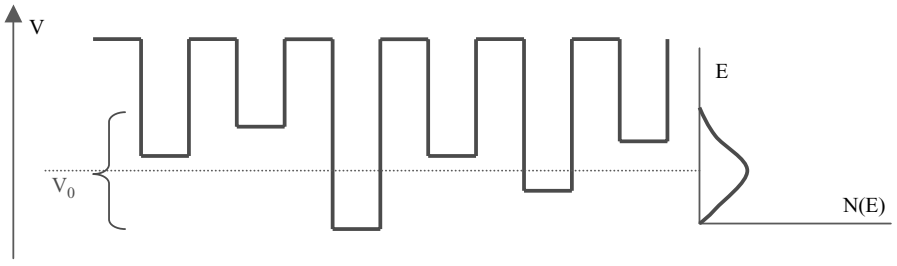

Figure II-11. Distribution of randomly deep potential wells.

distribution of wells with depth such that $|\Omega|_{moy} = (V_0/2)$, we obtain:

$$\frac{1}{\mathcal{L}} = \frac{P_{nm}}{v} = \frac{1}{4}\frac{2\pi}{\hbar}\left(\frac{V_0}{2}\right)^2 a^3 \frac{N(E_F)}{v}, \tag{24}$$

in which $N(E_F)$ is the density of states at the Fermi level and v the velocity of an electron at the Fermi level.

As $\mathcal{L}$ is large, the system under consideration is almost a perfect crystal and therefore we can write:

$$N(E) = \frac{4\pi(2m^*)^{3/2}E^{1/2}}{h^3} \text{ and } v = \left(\frac{2E}{m^*}\right)^{1/2}.$$

In using the effective mass given in eqn (22), eqn (24) gives:

$$\frac{a}{\mathcal{L}} = \frac{(V_0/\beta)^2}{32\pi}; \quad \text{and with} \quad B = 2ZI, \frac{a}{\mathcal{L}} = \frac{(2ZV_0/B)^2}{32\pi}. \tag{25}$$

— *System in which $(V_0/B) \approx 1$ (single disorder value) corresponding to $\mathcal{L} \approx a$ for weak disorder*

When $\mathcal{L} \approx a$, eqn (25) written for a cubic system in which $Z = 6$ results in $(V_0/B) = 0.83 \approx 1$. At this point when $\mathcal{L} \approx a$ (and $V_0 \approx B$), the disorder is such that $\Delta k \approx k$ (following Ioffe and Regel), and under such conditions, at each collision, k randomly varies by Δk, the closest neighbour to k. In going from one potential well to the next, the wavefunction as detailed in eqn (23) randomly changes and, following Mott, looses its phase memory and should therefore be rewritten using an approximate form:

$$\psi_k(r) = \sum_n A_n \psi_0(r - r_n),$$

with $A_n = c_n \exp(i\varphi_n)$, in which A_n is a function with a random phase and a near constant amplitude. Moreover, this amplitude is more constant than the variation between neighbouring potential wells *i.e.* V_0 is low. In a model using two wells with potential depths V_1 and V_2 (as in Miller and Abrahams [Mil 60]) the resulting wavefunction can take on either a symmetrical or antisymmetrical form, respectively, $\psi_S = A_1\psi_1 + B\psi_2$ or $\psi_A = A_1\psi_1 - B\psi_2$. We can therefore show that when $|V_1 - V_2| \ll |\beta|$ (*i.e.* V_0 is low), so $A_1 \approx A_2$, the difference in energy $(E_1 - E_2)$ between the two possible states is such that $|E_1 - E_2| \approx 2|\beta|$ [Mot 79] and [Mol 91]. A representation of the function is shown in Figure II-2-a for a network of several potential wells.

— *System in which $(V_0/B) > 1$ ((V_0/B) just above single order value): initial delocalisation and medium disorder*

In a system which corresponds to a great increase in disorder, and for the model of just two wells would correspond to an increase in the depth between the wells as in $|V_1 - V_2| = V_0$, the difference in energy, $|E_1 - E_2|$, increases to a corresponding level and A_1 differs from A_2. The amplitudes of the functions are no longer constant and the wavefunction displays increasing disorder both in amplitude and in phase (Figure II-12-b).

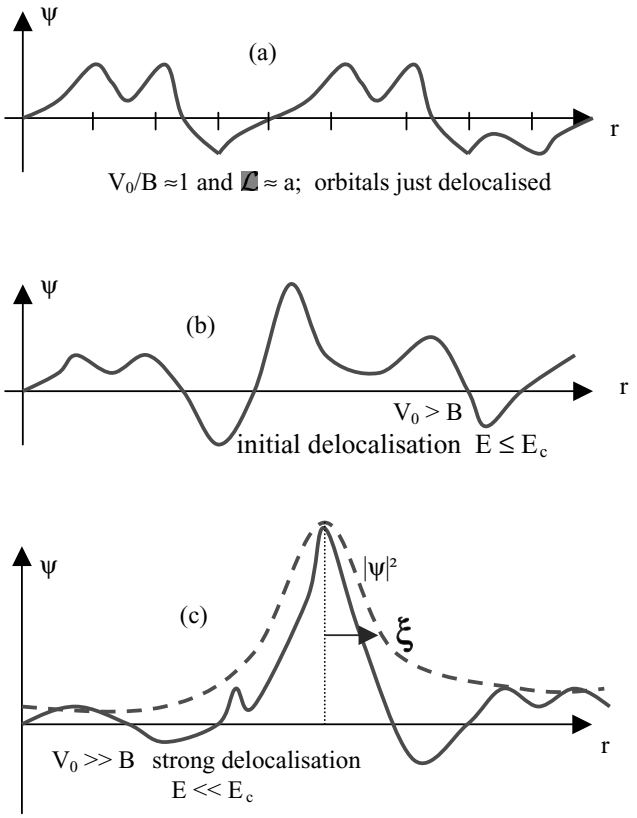

Figure II-12. Variations in wavefunction with delocalisation: (a) delocalisation—localisation only; (b) weak delocalisation; and (c) strong delocalisation.

— *System in which* $(V_0/B) \gg 1$*((*V_0/B*) well above single order value): strong delocalisation and great disorder*

In this system a highly localised state is formed, as shown in Figure II-12-c, and as V_0 increases the localisation is accentuated. In addition, there is no longer propagation along a line of potential wells and states are thus localised. An exponential decrease in the wavefunction starts to appear and is increasingly noticeable with increasing values of V_0. The wavefunction takes on the form

$$\psi(r) = \left[\sum_n A_n \psi_0(r - r_n)\right] e^{-\alpha r}$$

and can be rewritten

$$\psi(r) = \left[\sum_n A_n \psi_0(r - r_n)\right] e^{-r/\xi},$$

in which ξ is the localisation length.

To conclude, the factor V_0/B is a crucial term in deciding whether only localised states form ($V_0/B > 1$) or whether both localised and delocalised states can co-exist ($V_0/B \leq 1$).

γ-*Band scheme and form of the states density function N(E)* From a realistic scheme of the distribution of potential wells, we can see that states should be localised within one energy domain and delocalised in another. Accordingly, in Figure II-13 is described a system with non-negligible disorder:

— all states at the tail end of the function N(E) which correspond to a high enough value of V_0 and from energies $E\langle E_c \text{and} E\rangle E'_c$ appear localised as before in the scheme of potential wells;
— however, the middle of the band corresponds to shallow states with small V_0, such as V_0/B, and is a zone of delocalised states which have $E'_c < E < E_c$.

d Localised states, conductivity and Anderson's metal-insulator transition

α-*Mott's definition*: Mott's definition is based on continuous conductivity relative to electrons with a given energy ($\sigma_E(0)$) and delocalised states are on average, at $T = 0$ K, those for which $\sigma_E(0)$ is zero *i.e.* $\langle\sigma_E(0)\rangle = 0$. To arrive at an average though, all possible configurations which have the energy E need to be considered, and while some electrons may have a non-zero energy, the average over all possible states with the corresponding energy E gives zero as a result. These states and the mobility they represent are in effect thermally activated.

However, at $T = 0$ K, delocalised states average to give $\sigma_E(0) \neq 0$, that is to say metallic behaviour occurs.

β-*State properties* In Figure II-13, two types of states—localised and delocalised—are separated by energies E_c and E'_c which together are called the 'mobility

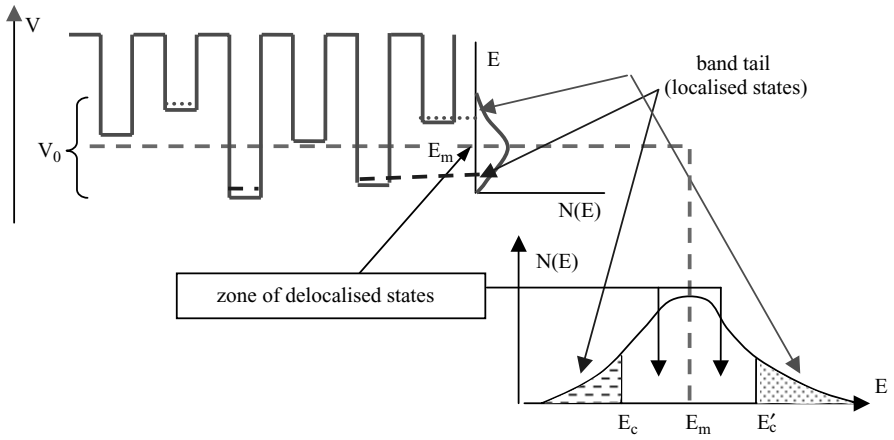

Figure II-13. Representation of localised and delocalised states co-existence.

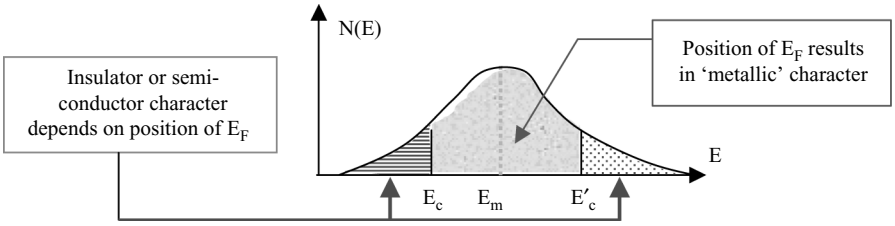

Figure II-14. Metallic character resulting from the domain E_F.

edge' . In the two zones Einstein's relation holds true if E_F is outside the bands of non-degenerate states. This gives $\mu = qD/kT$, but the diffusion coefficients (D) have different forms, as in $D = Pa^2$ in which P represents the probability of movement to neighbouring sites. This brings us to the origin of the expressions used in Chapter 5:

- when $E > E'_c$ and $E < E_c$, $D = (1/6)\nu_{ph}a^2 \exp(-w_1/kT)$ (with ν_{ph} being the phonon frequency and w_1 the energy of activation) and $\langle\sigma_E(0)\rangle_{T=0K} = 0$. Here as $T \to 0$, we can verify that D and μ tend towards zero, much as conductivity; and
- when $Ec < E < E'_c$, $D = (1/6)\nu_e a^2$ and $\sigma_E(0) \neq 0$ where ν_e is the frequency of electronic vibrations.

γ-*Slightly disordered media, in which localisation is slight and* $\mathcal{L}$ *is small, and the distinction between an insulator or semiconductor and a metal* As in the case of classic, crystalline media, the position of E_F, as detailed in Figure II-14, is related to the nature of a material. When E_F is situated in the domain of delocalised states ($E_c < E_F < E'_c$) there is degeneration appropriate for a 'metallic' character. However, when E_F is situated in the zone of localised states, for which typically $E < E_c$, charge carriers can only be thermally excited and conductivity can occur only by jumps or by excitation to Ec, and indeed at O K conductivity tends towards 0 which is typical of an insulator. Materials for which the Fermi level is situated in an energy zone in which states are localised are called Fermi glasses.

δ-*Metal-insulator or semiconductor transition* For a given material which has a Fermi level fixed by its charge density, displacement of E_C, for example by increasing the disorder as shown in Figure II-15, moves the Fermi level from an initial state in a domain of delocalised states (metallic) to a zone of localised states. The result is a metal to insulator or semiconductor transition.

ε-*Anderson transition from order to disorder and the change in conductivity* Even though we do not detail transport properties in this Chapter, we should nevertheless introduce an expression for metallic conductivity written in the relatively simple form of $\sigma = qn\mu = nq^2\tau/m^*$, in which n is electron concentration and τ is the relaxation time with respect to the Fermi level. With $\mathcal{L} = v\tau$ we have $\sigma = nq^2\mathcal{L}/m^*v$, and on introducing the crystalline momentum, $\hbar k = m^*v$, we reach $\sigma = nq^2\mathcal{L}/\hbar k_F$ in which k_F is the wave vector at the Fermi surface. We can also note that the number n of electrons within a unit volume V($V = 1$) can be obtained by use of the reciprocal space,

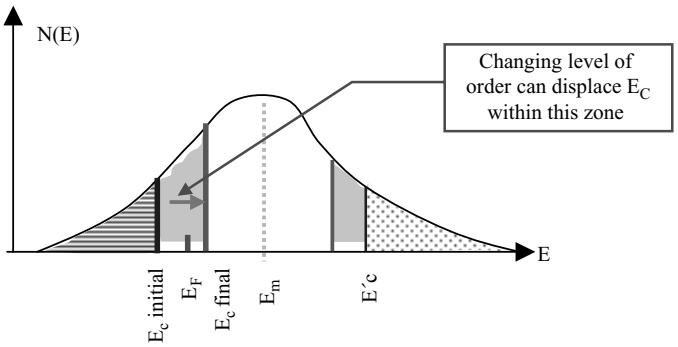

Figure II-15. Using disorder to displace E_C and effect metal-insulator transition.

that is to say the number of cells within the Fermi volume being $([4/3]\pi k_f^3)/8\pi^3$, each with volume $8\pi^3/V = 8\pi^3$ for $V = 1$. In taking into account electron spins (*i.e.* doubly occupied cells), we have $n = 2([4/3]\pi k_f^3)/8\pi^3$ and metallic conductivity can therefore be written as $\sigma_B = 4\pi k_F{}^2 q^2 \mathcal{L}/12\pi^3 \hbar$ (*cf.* Section III-1 in Chapter V).

When considering a metallic state, the Fermi level can be considered more or less at the band middle, as in 1-D with $k_F \propto \pi/a$ (p. 21 of [Mot 93]) and Figure II-14. With increasing disorder, E_c and E_c' tend towards each other at the band centre $E_M (\approx E_F)$ at which point all states are delocalised. This change is called Anderson's transition and is detailed in Figure II-16. Simultaneously, $V_0/B \geq 1$ with $\mathcal{L}$ tending towards a. For its part, with $\mathcal{L} = a$, conductivity σ tends towards $\sigma_{min} = \sigma_{IR} = (\sigma_B)_{\mathcal{L}=a} = q^2/3a\hbar$. In mono-dimensional media this abrupt transition is a point of controversy as it is known to occur progressively in 3-dimensions. When a is of the order of 3 Å, $\sigma_{IR} = 700\,S\,cm^{-1}$, often a saturation value for conductivity in rising temperatures.

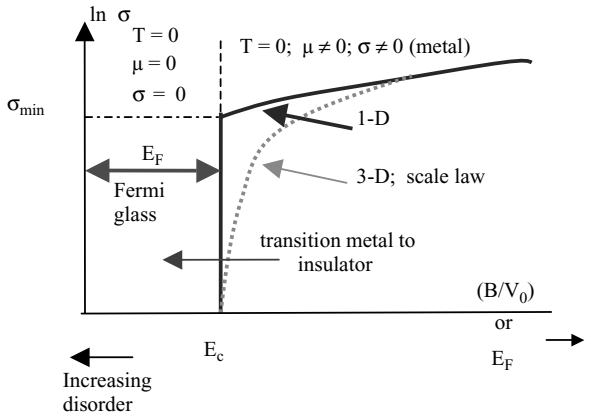

Figure II-16. Anderson's transition from metal to insulator at absolute zero following $1/(V_0/B) = B/V_0$. The same phenomena occurs as E_F is displaced from E_C.

V Conclusion

The origin of energy bands in a perfect three dimensional crystal, a material which presents a perfect regularity tied to a geometric structure unaltered by any physical reality was presented in this Chapter. In addition, supplementary effects such as dangling bonds, chain ends and holes within the structure were considered. These imperfections introduced into the band gap localised levels which once fluctuated could open to form a band which could split as a function of electron filling, in a manner analogous to the perturbations caused by electron repulsions, which were not taken into account in the band theory.

By introducing modifications of crystal regularity by considering network thermal vibrations (phonons) and defects, both chemical (impurities) and physical (dislocations), the notion of a real crystal was studied. This resulted in determining the free mean pathway of electrons, which could no longer be considered as completely delocalised within the network—as was the case in a perfect crystal. It was shown that an increase in disorder reduced the free mean path length up to the point of localising

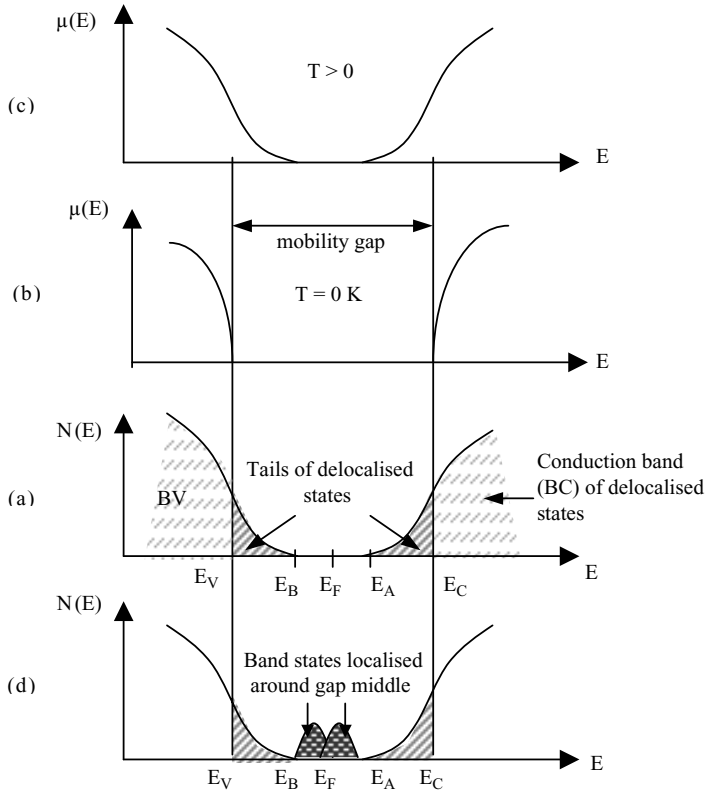

Figure II-17. Band models for amorphous semiconductors: (a) following CFO; (b) following μ(E) at T = 0 K; (c) following μ(E) at T > 0 K; and (d) following that of Mott and Davis.

electrons in neighbourhoods of deep defaults, resulting in energy levels localised at extremities, or "tails", of permitted bands.

Finally, it can be noted that all models postulate for amorphous media such as crystalline semiconductors that there are conduction and valence bands which are or are not separated by a band gap, depending on the all important band tails. And that:

— bands result in part from short range order (from approximations of strong bonds giving rise to bonding and anti-bonding states, *i.e.* valence and conduction bands separated by a band gap) and from disorder created by phonons or impurities shown by tails of delocalised states. Tail states are neutral when occupied in the case of the valence band and when empty in the conduction band. The Fermi level is thus placed in the middle of the band gap, as shown in Figure II-17 and following the model proposed by Cohen, Fritzsche and Ovshinsky (CFO).
— the form of the bands depends on the type of the implicated orbitals. For p or d orbitals, which are less stretched overall into space than s-orbitals, the form of N(E) is different and the bands are smaller.
— in a perfect crystal, the band gap is an forbidden energy in which $N(E) = 0$, while in an amorphous material it is a mobility gap and N(E) is not necessarily zero but the mobility $\mu(E)$ however does becomes zero at $T = 0\,K$ (localised states), as shown in Figure II-17-b and c.

By taking into account the disorder caused by not only phonons and impurities but also by structural defects such as dangling bonds and chain ends, additional offsetting defaults localised in the middle of the band can generate two bands at compensating levels (Hubbard's bands) following the model of Mott and Davis as shown in Figure II-17-d.

http://www.springer.com/978-0-387-23710-7

Optoelectronics of Molecules and Polymers

Moliton, A.

2006, XXXI, 498 p. 229 illus., Hardcover
ISBN: 978-0-387-23710-7